Received June 24, 2019, accepted July 8, 2019, date of publication July 10, 2019, date of current version July 25, 2019.

Digital Object Identifier 10.1109/ACCESS.2019.2928057

On the Reliable Localization of WiFi Access Points

JUSHANG SHEN[1], BAOQI HUANG[1], (Member, IEEE), YU TIAN[1], AND LONG ZHAO[2]
[1]College of Computer Science, Inner Mongolia University, Hohhot 010021, China
[2]School of Automation Science and Electrical Engineering, Beihang University, Beijing 100191, China

Corresponding author: Baoqi Huang (cshbq@imu.edu.cn)

This work was supported in part by the National Science and Technology Major Project of the Ministry of Science and Technology of China under Grant 2016YFB0502102, in part by the National Natural Science Foundation of China under Grant 41871363, Grant 61461037, Grant 41761086, and Grant 61761035, in part by the Natural Science Foundation of Inner Mongolia Autonomous Region of China under Grant 2017JQ09, and in part by the ''Grassland Elite'' Project of the Inner Mongolia Autonomous Region under Grant CYYC5016.

ABSTRACT Acquiring the locations of WiFi access points (APs) not only plays a vital role in various WiFi related applications, such as localization, security and AP deployment, but also inspires the emergence of novel applications. Thus, many efforts have been invested in studying AP localization. Most existing studies adopt the well-known lognormal distance path loss (LDPL) model, which only accounts for large-scale fading but ignores small-scale fading induced by multipath propagation. In this paper, we tackle the problem of AP localization based on the Rayleigh lognormal model which characterizes the influence of both large-scale fading and small-scale fading. In addition, particle filtering is used to sequentially narrow the scope of possible locations of the target AP. In order to label the locations of received signal strength (RSS) measurements in real time, manual configuration or certain indoor and outdoor localization techniques, including GPS, pedestrian dead reckoning (PDR) and WiFi fingerprinting, can be leveraged. Moreover, due to the bias caused by unavailable or inaccurate state space, a particle area dynamic adjustment strategy (PADAS) is designed to improve the AP localization accuracy. Extensive experiments were carried out in typical indoor and outdoor scenarios. It is shown that, if accurate location labels are available, the proposed method is able to achieve an average localization accuracy of 2.48 m indoors and 4.21 m outdoors. In comparison with the LDPL based solutions, the proposed method improves by 23.82% – 70.38% indoors and 14.13% – 35.94% outdoors; more importantly, the proposed method enhanced by using PDR, PADAS, GPS and WiFi fingerprinting can achieve localization accuracy comparable to that with accurate location labels. In addition, an Android application (APP) was developed to demonstrate the feasibility of the proposed algorithm on smartphones.

INDEX TERMS WiFi access points localization, Rayleigh lognormal model, particle filtering, pedestrian dead reckoning.

I. INTRODUCTION

With the popularization of IEEE 802.11 networks, various novel services and products have been spurred [1]–[3], and WiFi access points (APs) have been ubiquitous in cities. Therefore, acquiring the knowledge of the locations of massive WiFi APs can contribute to various applications [4]–[7]. For example, the locations of nearby WiFi-enabled mobile devices can be inferred with the locations of APs via, e.g. trilateration, after converting received signal strength (RSS) measurements to distances [8], [9]; GPS-free outdoor localization solutions can be available when using the locations of APs [10]; the locations of APs can also help to localize malicious AP or deploy new APs [11].

Most existing studies [12]–[16] employed the lognormal distance path loss (LDPL) model to localize WiFi APs. However, the LDPL model only accounts for large-scale fading but ignores small-scale fading induced by multipath propagation. In a complex real environment such as indoor offices and urban commercial districts, the multipath effect is very serious and can influence the results of signal reception a lot [17]. Moreover, a few studies [18], [19] established some empirical models to replace the LDPL model, but the accuracy of AP localization was quite limited. In addition, by asking a user to walk and rotate, an interactive approach was presented in [20] to determine the direction of an AP.

Consider localizing a target AP through a crowdsourcing approach in the following scenario: when a user walks by carrying a smartphone, his/her locations can be determined through manual configuration or some localization techniques, e.g. GPS in outdoor environments, WiFi fingerprinting in indoor environments and so on [21], [22]; during the period of walking, the smartphone automatically and continuously collects RSS measurements of beacon packets

The associate editor coordinating the review of this manuscript and approving it for publication was Shuai Han.

from the target AP; after that, the location of the target AP can be estimated in real time and further leveraged in various fields. To do so, one has to address two critical issues, namely how to label the location of each RSS measurement as precise as possible and how to accurately infer the AP location by using a sequence of RSS measurements from this AP.

In this paper, we tackle the above two issues from the following aspects. First, instead of the LDPL model, a more practical Rayleigh lognormal model that reflects both large-scale and small-scale fading [23] is adopted to characterize the relationship between RSS measurements and corresponding distances. Given that the wireless channel between an AP and a mobile device is often non-line-of-sight (NLoS) in both indoors and outdoors, it is evident that the Rayleigh lognormal model is more suitable than the Rician fading model which considers line-of-sight (LoS) channels. Second, since the RSS measurements arrive sequentially, the AP localization problem is formulated as a particle filtering optimization problem [24], [25]. Third, GPS and WiFi fingerprinting are used to respectively obtain the location labels of RSS measurements in outdoor and indoor scenarios. In order to further improve the localization accuracy, PDR is adopted. Fourth, since the localization estimates of APs severely suffer from biases, a particle area dynamic adjustment strategy (PADAS) is presented to mitigate the bias influence. Finally, extensive experiments were conducted in both typical indoor and outdoor scenarios. It is shown that the proposed method significantly outperforms existing methods. In addition, an Android application (APP) was developed to confirm that it is totally acceptable to apply the proposed method in practice. Part of the content in this paper has been reported in [26].

The rest of this paper is organized as follows. In Section II, the literature is briefly reviewed. In Section III, given an ideal scenario where location labels are accurate, the proposed method is elaborated based on the Rayleigh lognormal model and particle filtering. In Section IV, given practical scenarios, the improvements of the proposed method are presented in detail. In section V, the experiments are conducted to verify the proposed method and its improved version. Section VI finally draws the conclusions and sheds lights on future works.

II. RELATED WORKS

In the literature, efforts for AP localization have been made. Most existing studies were conducted based on the well known LDPL model [12]–[15].

In [12], a method called AP_Area was proposed to infer the location of a target AP. This method obtained the propagation parameters of the LDPL model offline, and acquired the locations of RSS measurement points by GPS. Only simulations were conducted and the results showed that the cumulative probability of positioning error less than 5 m is 80% (RSS distortion was set to be less than 20%).

In [13], the weighted nonlinear least square (NLS) was used to simultaneously infer the propagation parameters of the LDPL model and the location of a target AP. Besides, a multi-level quality control mechanism was proposed to further improve the performance of this method. Experiments were carried out in an indoor environment and the results indicated that the localization accuracy was improved by 47% $\sim$ 86% compared to the previous LDPL-based methods.

Ji *et al*. used the Monte Carlo simulation method to estimate the location of a target AP and the propagation parameters of the LDPL model [14]. Both simulations and experiments in an office building were conducted and showed that the localization errors were around 10 m with a 95% confidence interval.

In order to reduce the costs of collecting RSS measurements, the Taylor expansion and Lagrange's method with crowdsourcing RSS measurements were adopted in [15]. The results of experiments showed that the average accuracy of AP localization was as good as 4 m. However, the good result is partly due to the fact that the path where RSS measurements were collected was very close to the target AP's real location [27], [28].

In addition, some other methods didn't adopt the LDPL model. Koo *et al*. established a linear relationship between RSS measurements and distances to replace the LDPL model, but the accuracy of AP localization was quite limited [18]. In [19], a modified Hata-Okumara model was applied and experimental results suggested that, if the positions of RSS measurements were carefully selected, the AP localization accuracy could be improved compared to the method mentioned in [18], but the improvement was limited too.

In summary, although different signal propagation models and various optimization methods are used in the existing works, AP localization still can not be effectively applied in practical applications due to its accuracy and environmental limitations. Therefore, this paper tackles this problem by using the Rayleigh lognormal model and particle filtering, and aims to improve the accuracy and feasibility of AP localization.

III. METHODOLOGY

In this section, we suppose that accurate location labels are available, and will elaborate the basic methodology.

A. RAYLEIGH LOGNORMAL MODEL

The Rayleigh lognormal model used in this paper are briefly introduced in this subsection.

Different from the LDPL model, the Rayleigh lognormal model can both take into account large-scale fading and small-scale fading. In [23], the probability density function of Rayleigh lognormal model can be approximated by

$$p(\mu_c) = \frac{4}{\Gamma(m_s)} h^{m_s+1} \mu_c^{m_s} K_{m_s-1}(2\mu_c h), \tag{1}$$

where μ_c is the signal amplitude at the receiver, $\Gamma(\cdot)$ is a Gamma function, $K_v(\cdot)$ is the modified Bessel function of the second kind and order v and m_s inversely reflects the shadowing severity.

By letting σ be the standard deviation of the shadowing effect (satisfying $\sigma = \sigma_{dB} \ln 10/10$) and $\overline{P_r}$ be the area mean power (namely that both the shadowing and multipath effects are averaged out) at a specific position, define

$$m_s = \frac{1}{e^{\sigma^2} - 1}, \tag{2}$$

$$\Omega_s = \overline{P_r}\sqrt{\frac{m_s + 1}{m_s}}, \tag{3}$$

$$h = \sqrt{\frac{m_s}{\Omega_s}}, \tag{4}$$

$$\overline{P_r} = \overline{P_r(d_0)} - 10n\log_{10}(\frac{d}{d_0}), \tag{5}$$

where Ω_s is the gamma shadow area mean power [23]. Then, according to [29], the instantaneous signal power, denoted P_r, can be expressed as

$$P_r = \frac{1}{2}\mu_c^2. \tag{6}$$

B. AP LOCALIZATION BASED ON PARTICLE FILTERING

First, define $\mathbf{s}_i$ to be the state at time instance i, $s_i^k = \{x_i^k, y_i^k, n_i^k, \sigma_i^k, r_i^k\}$ and w_i^k to be the k-th particle and its weight with $k = 1, \cdots, N$, where $[x_i^k, y_i^k]$ is the location coordinates, n_i^k is the path loss exponent, σ_i^k is the standard deviation of the shadowing effect, and r_i^k is the average received power at reference distance d_0 which is set to be 1 m without loss of generality. Let m_i be the observation at time instance i, namely the RSS measurement from the target AP.

In particular, the initial state $\mathbf{s}_0$ can be obtained by sampling the random and uniform distribution based on the priori knowledge of the spatial and channel characteristics, and the corresponding weight $w_0^k = 1/N$. Given the RSS measurement at each time instance, say m_i, the weight w_i^k can be updated by

$$\hat{w}_i^k = w_{i-1}^k \times p(\mu_c), \tag{7}$$

where μ_c and $p(\mu_c)$ can be calculated by using (6) and (1). Then, the weights are normalized as below

$$w_i^k = \frac{\hat{w}_i^k}{\sum_{j=1}^N \hat{w}_i^j}. \tag{8}$$

The location estimate can be calculated in a weighted average manner as follows

$$[\hat{x}_i, \hat{y}_i] = \sum_{k=1}^N w_i^k \times [x_i^k, y_i^k]. \tag{9}$$

An importance sampling step is initiated based on the Bayesian bootstrap to avoid particle degradation [30]

$$\frac{1}{\sum_{k=1}^N (w_i^k)^2} < \frac{2N}{3}. \tag{10}$$

Repeat the above steps until there is no more RSS measurement. Finally, $[\hat{x}_i, \hat{y}_i]$ is returned as the location estimate of the target AP, and we call the proposed method RP as described in Algorithm 1.

Algorithm 1 The RP Algorithm

Input: The set of RSS measurements before time instance q, denoted m_i with $i = 1, \cdots, q$; the corresponding location labels, denoted (X_i, Y_i); the particle's area, denoted PA, and the particle's number, denoted N;
Output: The estimated position of the target AP, denoted $[\hat{x}_q, \hat{y}_q]$; the path loss exponent, denoted n_q; the standard deviation, denoted σ_q; the average received power at 1 m, denoted r_q;
Let $\mathbf{s}_i$ to be the state at time instance i, $s_i^k = \{x_i^k, y_i^k, n_i^k, \sigma_i^k, r_i^k\}$ and w_i^k to be the k-th particle and its weight with $k = 1, \cdots, N$;
Initialize $\mathbf{s}_0$ by sampling according to a random and uniform distribution in PA, and the corresponding weight $w_0^k = 1/N$;
for each m_i and (X_i, Y_i), **do**
  for each s_{i-1}^k, **do**
    Calculate $p(\mu_c)$ using the Rayleigh lognormal model;
    Update the weight $\hat{w}_i^k = w_{i-1}^k \times p(\mu_c)$;
  end for
  for each $\hat{w}_i^k$, **do**
    Normalize the weight $w_i^k = \frac{\hat{w}_i^k}{\sum_{j=1}^N \hat{w}_i^j}$;
  end for
  if $\frac{1}{\sum_{j=1}^N \left(w_i^j\right)^2} < \frac{2}{3}N$, **then**
    Break;
  end if
  Resampling;
  for each w_i^k, **do**
    Update the weight $w_i^k = \frac{1}{N}$;
  end for
end for
Caculate $[\hat{x}_q, \hat{y}_q]$, n_q, σ_q and r_q using the weighted average method;
Return $[\hat{x}_q, \hat{y}_q]$, n_q, σ_q and r_q.

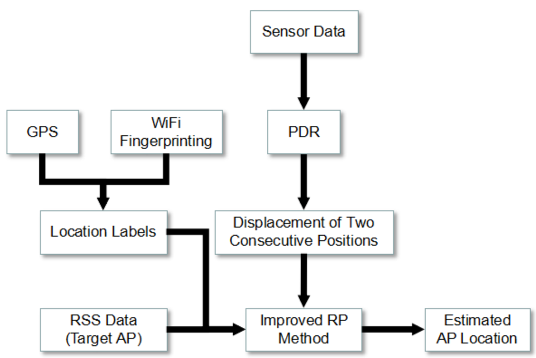

FIGURE 1. System architecture.

IV. ENHANCING THE AP LOCALIZATION METHOD

The overall system architecture is depicted in Fig. 1. As can be seen, GPS and WiFi fingerprinting are used to obtain the location labels of RSS measurements; PDR is employed to further improve the localization accuracy; finally, the improved RP method based on PADAS is applied to fuse the above information in the estimation of AP location.

A. PDR

PDR generally involves estimating three critical quantities, namely step length, heading and step count. In order to estimate the step length of a user, the method proposed by Shin et al is used [31]; the yaw angle mentioned in [32] is calculated to decide the heading; the fast Fourier transform (FFT) based step detection and counting method proposed in [33] is used to obtain the step count. After obtaining the estimates of the step length, heading and step count, the displacement of two consecutive positions can be calculated.

We improve the RP method by incorporating the displacement information into the particle filtering. The particle's state is extended with $[X_i^k, Y_i^k]$ which denotes the approximate location label used for calculating $p(\mu_c)$, and is updated according to the location label at the previous time instance, displacement information and current localization result, namely

$$[X_i^k, Y_i^k] = \frac{[X_{i-1}^k, Y_{i-1}^k] + [D_{Xi}, D_{Yi}] + [X_i, Y_i]}{2}, \quad (11)$$

where $[D_{Xi}, D_{Yi}]$ is the displacement at time instance i; $[X_i, Y_i]$ is the localization result returned by, e.g. GPS or WiFi fingerprinting, at time instance i. The improved RP algorithm is described in Algorithm 2.

Algorithm 2 The Improved RP Algorithm

Input: m_i; (X_i, Y_i); PA and N; the displacements, denoted (D_{Xi}, D_{Yi}); $i = 1, \cdots, q$;
Output: $[\hat{x}_q, \hat{y}_q]$; n_q; σ_q; r_q;
Let $\mathbf{s}_i$ to be the state at time instance i, $s_i^k = \{x_i^k, y_i^k, n_i^k, \sigma_i^k, r_i^k, X_i^k, Y_i^k\}$ and w_i^k to be the k-th particle and its weight with $k = 1, \cdots, N$;
Initialize $\mathbf{s}_0$ by sampling according to a random and uniform distribution in PA, X_0^k and Y_0^k are generated according to random and normal distributions based on the initial location label, and the corresponding weight $w_0^k = 1/N$;
for each m_i, (X_i, Y_i) and (D_{Xi}, D_{Yi}), **do**
  Update (X_i^k, Y_i^k) according to (X_{i-1}^k, Y_{i-1}^k), (D_{Xi}, D_{Yi}) and (X_i, Y_i);
  for each s_{i-1}^k, **do**
    Calculate $p(\mu_c)$ using the Rayleigh lognormal model, and $\left(X_i^k, Y_i^k\right)$ is used to replace (X_i, Y_i);
    Update the weight $\hat{w}_i^k = w_{i-1}^k \times p(\mu_c)$;
  end for
  for each $\hat{w}_i^k$, **do**
    Normalize the weight $w_i^k = \frac{\hat{w}_i^k}{\sum_{j=1}^N \hat{w}_i^j}$;
  end for
  if $\frac{1}{\sum_{j=1}^N \left(w_i^j\right)^2} < \frac{2}{3}N$, **then**
    Break;
  end if
  Adjust particle area;
  Resampling;
  for each w_i^k, **do**
    Update the weight $w_i^k = \frac{1}{N}$;
  end for
end for
Caculate $[\hat{x}_q, \hat{y}_q]$, n_q, σ_q and r_q using the weighted average method;
Return $[\hat{x}_q, \hat{y}_q]$, n_q, σ_q and r_q.

B. PADAS

The localization results suffer from severe biases, which is attributed to the fact that the performance of the AP localization method based on particle filtering is greatly dependent on the area in which particles are distributed. Therefore, we propose the PADAS, including the initial particle area determination and particle area adjustment, to mitigate the bias influences, thereby enhancing the AP localization accuracy.

1) INITIAL PARTICLE AREA DETERMINATION

Given an arbitrary RSS measurement from a target AP, the distance between the location where the RSS measurement is made and the target AP can be roughly estimated as

$$\hat{d} = 10^{\frac{\overline{P_r(d_0)} - P_r}{10n}}. \quad (12)$$

However, the $\hat{d}$ is inaccurate according to [34]. Therefore, we set the $\overline{P_r(d_0)}$ and n to be -28 dBm and 2 to increase $\hat{d}$ appropriately, so that the target AP can be covered as possible. After that, a square initial particle area can be determined by letting the location label be its center and $2\hat{d}$ be the side length.

2) PARTICLE AREA ADJUSTMENT

Prior to resampling in Algorithm 2, the particle area is updated by generating a new square which is centered at the weighted average of AP location estimates in all the particles' states and a fixed number (say 30 m) as the side length. Based on the updated particle area, the resampling is implemented to generate new particles randomly and evenly. As shown in Fig. 2, the red dashed square represents the previous particle area, the blue dashed square represents the

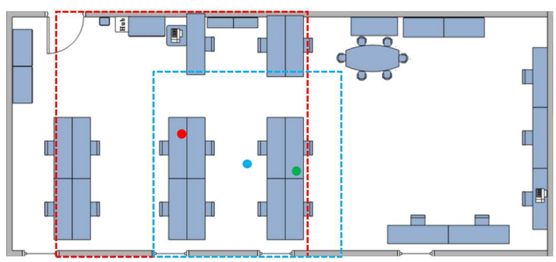

FIGURE 2. Particle area adjustment.

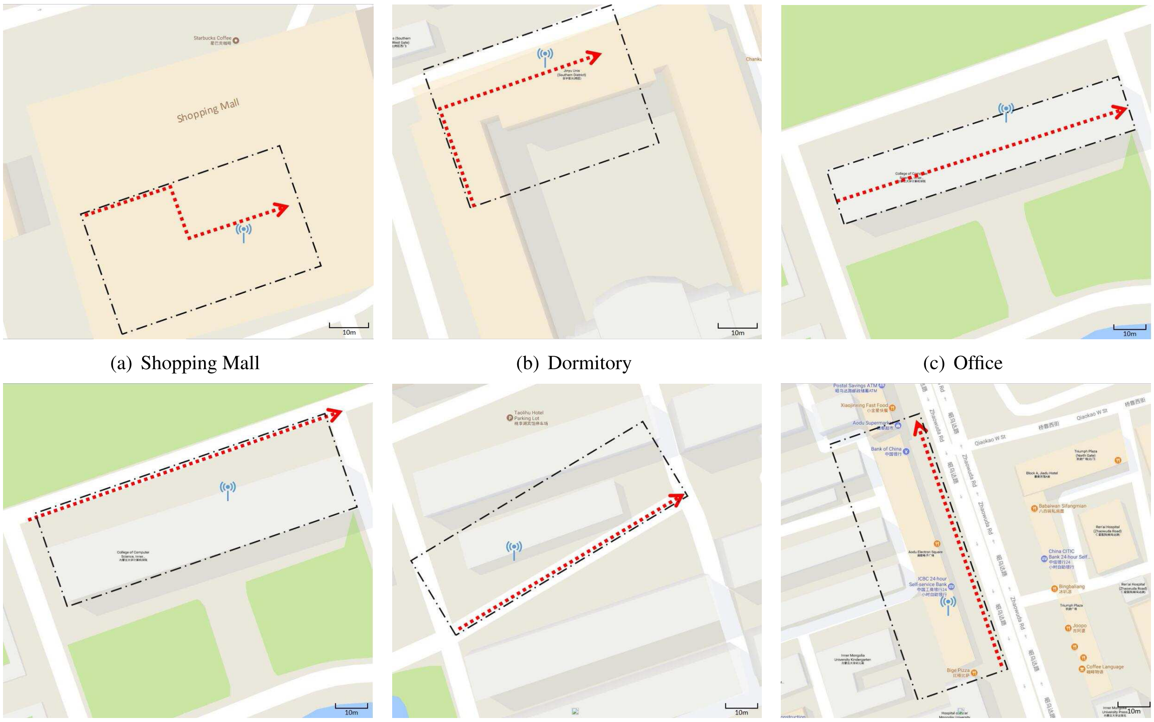

(a) Shopping Mall (b) Dormitory (c) Office

(d) Campus (e) Residential Area (f) Urban Street

FIGURE 3. The layout of the routes and buildings in the experiments.

updated particle area, the red and green dots represent the center of the red square and the true target AP position, the blue dot represents the weighted average result of AP location estimates in all the particles' states.

V. EXPERIMENTS

In this section, both indoor and outdoor scenarios are taken into consideration to verify the effectiveness of the proposed method and its improved version. In addition, the Android APP developed is used to validate the feasibility of the proposed method.

A. EXPERIMENTS WITH ACCURATE LOCATION LABELS

First of all, in order to evaluate the performance of the proposed method, we have carried out extensive experiments in typical indoor and outdoor scenarios by assuming that accurate location labels of RSS measurements are available.

1) EXPERIMENTAL SETUP

As shown in Fig. 3, the experiments were conducted in 6 typical scenarios. One WiFi AP was installed on a 1.5-meter high tripod placed in the position marked by a blue WiFi icon, and the routes where RSS measurements were collected are marked by red dotted lines. Two students (1 male and 1 female) were requested to walk along the specified route 5 times at constant speeds in each scenario.

Another two methods based on the LDPL model, termed LP (using particle filtering) and LN (using NLS), were implemented. As for the implementation of Particle Filtering, the particle number is set to be 5000, and the state space in each scenario is set to be a rectangle drawn in black dashed lines in Fig. 3.

2) LOCALIZATION PERFORMANCE

In the first place, the distributions of the localization errors produced by the three methods are depicted in Fig. 4. It's obvious that the proposed RP method is superior to the other two methods; moreover, it is clear that the proposed RP method incurs a small error variations compared to the other two methods, indicating that the proposed method is relatively stable.

Regarding to the 3 indoor scenarios, the localization errors in the Shopping Mall and Dormitory scenarios are much less than those in the Office scenario, which can be explicated in the following two dimensions: (1) the routes are closer to the target AP in the Shopping Mall and Dormitory scenarios compared to the Office scenario; (2) the curved routes in the Shopping Mall and Dormitory benefit AP localization according to the existing localization performance studies [35]. In addition, the average localization errors and the relative improvement are listed in Table 1 (including indoor scenarios) and Table 2 (including outdoor scenarios) to make a clear comparison.

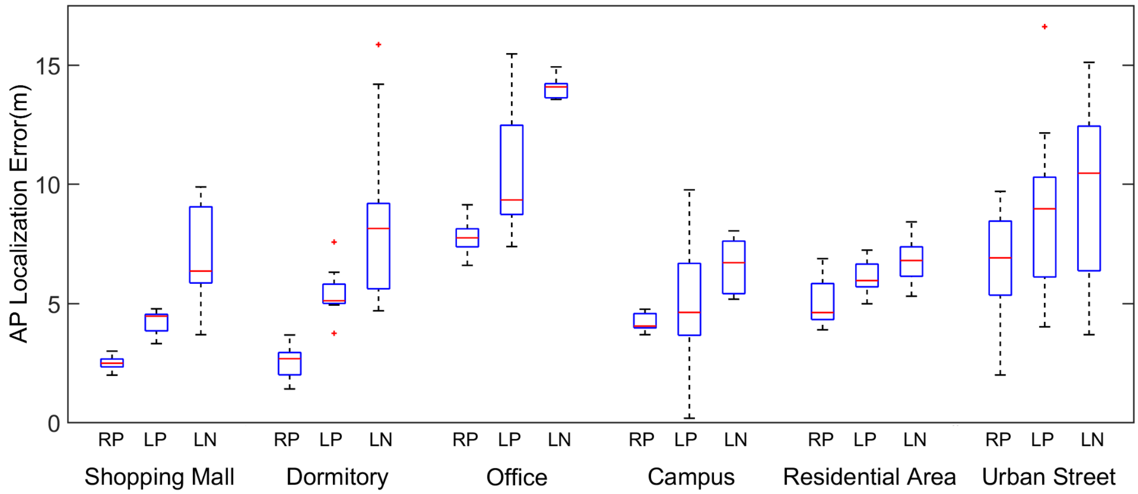

FIGURE 4. Location error distributions.

TABLE 1. The comparison of the mean localization errors in indoor scenarios.

	Shopping Mall		Dormitory		Office	
	Error (m)	Ratio (%)	Error (m)	Ratio (%)	Error (m)	Ratio (%)
RP	2.4766	-	2.5553	-	7.8019	-
LP	4.2446	41.65	5.4028	52.70	10.2418	23.82
LN	6.9941	64.59	8.6258	70.38	14.0684	44.54

TABLE 2. The comparison of the mean localization errors in outdoor scenarios.

	Campus		Residential Area		Urban Street	
	Error (m)	Ratio (%)	Error (m)	Ratio (%)	Error (m)	Ratio (%)
RP	4.2088	-	5.0256	-	6.6055	-
LP	4.9012	14.13	6.1256	17.96	8.7841	24.80
LN	6.5701	35.94	6.7620	25.68	9.6143	31.30

Therefore, it can be concluded that the proposed RP method surpasses the other two LDPL based methods, and the results of experiments agree with the advantages of the Rayleigh lognormal model.

3) THE EFFECT OF THE PARTICLE NUMBER

The localization errors of different particle densities (equal to the average number of particles in 1 m^2) produced by the proposed method RP in the office scenario are depicted in Fig. 5. As can be seen, there is no more significant improvement in localization accuracy when increasing the particle number beyond 1 particle per squared meter. Similar results can be observed in other scenarios. On these grounds, the particle density adopted in our following experiments is 1 m^{-2} with the result that the particle number is less than 10000 if the particle area is maximally 100×100.

B. EXPERIMENTS WITHOUT ACCURATE LOCATION LABELS

In order to validate the improved method, we first conduct experiments only in the outdoor urban street due to the

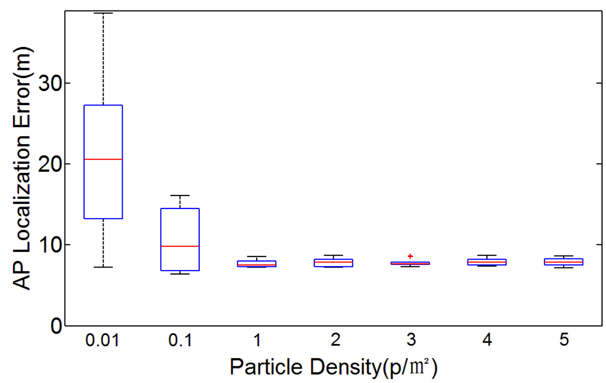

FIGURE 5. The location error distributions of different particle densities.

difficulties in aligning outdoor coordinate systems; then, we carry out experiments in the indoor office scenario where the WiFi fingerprint-based localization system is available for approximately determining the location labels of RSS measurements.

1) OUTDOOR EXPERIMENTS

As shown in Fig. 3(f), outdoor experiments are carried out in the urban street. One WiFi AP (ASUS RT-N16) was installed on a 1.5-meter high tripod placed in the position marked by a blue WiFi icon, and the route along which RSS measurements from the target AP were collected is marked by a red dotted line. 5 participants (3 males and 2 females) held the same smartphone and walked along the specified path twice to collect data.

In order to obtain the true coordinate of the target AP which is placed inside a shop, an indirect approach was adopted due to the unavailability of GPS for indoor environments. First, we collect GPS data at a selected outdoor position for 5 minutes and average the collected data; then, the distance and direction from the outdoor position to the target AP are measured by using a ruler and a compass; finally, by combining the measurements above, the true coordinates of the target AP can be obtained.

In order to evaluate the performance of every part of the improved method, we implement the following four different versions: the RP-G (using the RP method and GPS), the RP-GA (including the PADAS into the RP-G), the RP-GD (including PDR into the RP-G) and the RP-GDA (including the PADAS into the RP-GD).

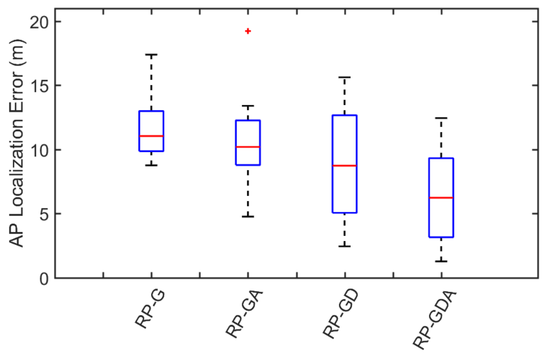

FIGURE 6. The location error distributions of outdoor experiments.

TABLE 3. The comparison of the mean localization errors in the outdoor urban street.

	Error (m)	Ratio (%)
RP-G	11.78	-
RP-GA	10.87	7.72
RP-GD	8.82	25.13
RP-GDA	6.57	44.23

The boxplots of the localization errors produced by the four methods are shown in Fig. 6. It can be observed that the introduction of the PADAS and PDR can substantially improve the AP localization results. To make a clear comparison, the average localization error and the relative improvement are listed in Table 3. It can be seen that the improvement ratio by PDR is 25.13%, while that by PADAS is only 7.72%. The reason why the improvement of PADAS is not significant is because the bias caused by the initial particle area is sufficiently small, such that there is no more need to reduce the bias. When the PADAS and PDR are introduced together, the average localization error can be as low as 6.57 m, and the improvement ratio is 44.23%.

Therefore, we can conclude that the enhanced method can effectively improve the AP localization accuracy of the RP method in the outdoor urban street scenario.

2) INDOOR EXPERIMENTS

In order to validate the improved method in indoor scenarios, we conduct experiments in the typical indoor office where the WiFi fingerprint-based localization system is available. As shown in Fig. 7, the office in Fig. 3(c) is partitioned into Office A, Office B and Office C. It should be noted that the WiFi fingerprint-based localization system achieves the localization accuracy between 2 m and 4 m.

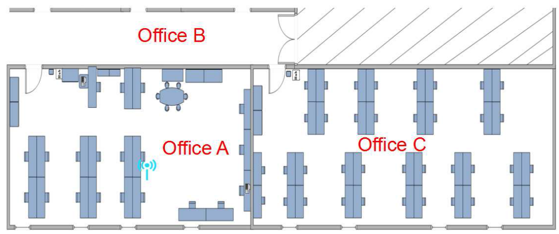

FIGURE 7. The indoor layout in experiments.

In the indoor experiments, one WiFi AP (ASUS RT-N16) was placed at the position marked by a blue WiFi icon, and 5 participants (3 males and 2 females) were asked to hold the same smartphone and walk around in each area (e.g., Office A, Office B and Office C) to collect two sets of RSS measurements from the target AP.

Similar to the outdoor experiments, we compare the RP-F (using the RP method and WiFi fingerprint-based localization), the RP-FA (including the PADAS into the RP-F), the RP-FD (including PDR into the RP-F) and the RP-FDA (including the PADAS into the RP-FD).

The boxplots of the localization errors produced by the four methods are shown in Fig. 8. It can be observed that the introduction of PDR and the PADAS can both reduce the AP localization errors. To make a clear comparison, the average localization errors and the relative improvement are listed in Table 4. It can be seen that, after introducing the PADAS, the average localization error can be as low as 3.52 m, and the improvement ranges between 22.98% and 52.59%; after introducing PDR, the average localization error can be as low as 3.66 m, and the improvement ranges between 19.91% and 39.02%; after introducing both the PADAS and PDR, the average localization error can be as low as 2.47 m, and the improvement ranges between 45.95% and 65.92%.

Therefore, we can conclude that the enhanced method can effectively improve the AP localization accuracy of the RP method in the indoor office scenario.

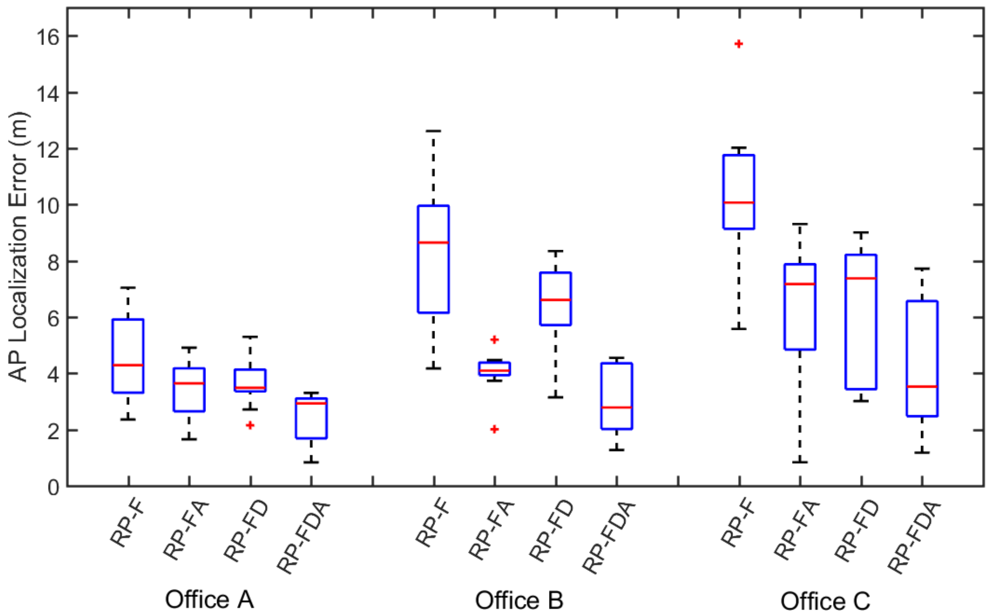

FIGURE 8. The location error distributions of indoor experiments.

TABLE 4. The comparison of the mean localization errors in the indoor office.

	Office A		Office B		Office C	
	Error (m)	Ratio (%)	Error (m)	Ratio (%)	Error (m)	Ratio (%)
RP-F	4.57	-	8.48	-	10.20	-
RP-FA	3.52	22.98	4.02	52.59	6.39	37.35
RP-FD	3.66	19.91	6.46	23.82	6.22	39.02
RP-FDA	2.47	45.95	2.89	65.92	4.36	57.25

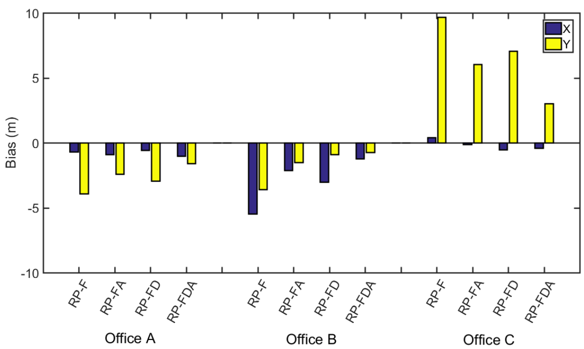

FIGURE 9. The biases of AP localization results.

Besides, the biases of AP localization results produced by the four methods are shown in Fig. 9. It can be observed that the PADAS can effectively reduce the biases, thereby reducing the AP localization errors; additionally, PDR also helps to reduce the biases, but the reduction is not as significant as the PADAS.

C. ANDROID APP

In order to confirm that the proposed method can be deployed in practice, we have developed an Android APP named L-AP based on Baidu MAP API. After starting L-AP, one can select a target AP from the list of surrounding APs, and configure three key parameters, including the RSS sampling interval, the number of particles and the range of AP localization; after that, RSS measurements and GPS data can be automatically and continuously collected, and then, the AP's estimated location can be updated and displayed.

By setting the sampling interval to be 1 s, the number of particles 5000 and the range 80m $\times$ 80m, the localization results of the AP at 1 s, 5 s and 30 s are illustrated in Fig. 10. In each figure, the blue dot denotes the current position of a participant, the red dot denotes the estimated location of target AP and the green dot which is drawn by us denotes the true AP location. It can be observed that, with the increasing number of RSS measurements, the location estimate of the target AP approaches to the true AP location; specifically, at 5 s, the localization error is around 10 m.

Furthermore, we evaluate the time efficiency of the proposed algorithm with respect to different numbers of particles on a smartphone. To be specific, the smartphone used is Xiaomi MI 8 SE with Snapdragon 710, 6GB RAM and 64GB storage. Given a specific number of particles, 10 sequences of RSS measurements are fed into the algorithm and the average

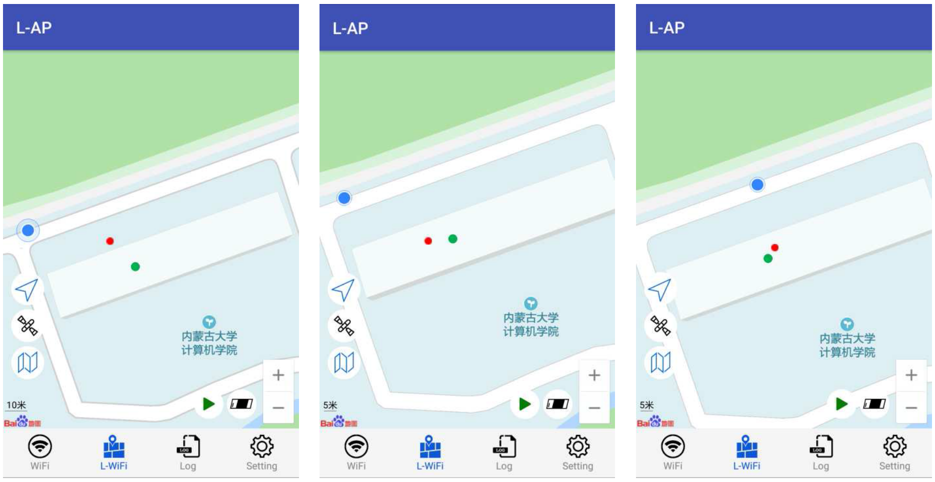

(a) 1 second (b) 5 seconds (c) 30 seconds

FIGURE 10. The displays of different moments in L-AP.

TABLE 5. The time costs with respect to different numbers of particles.

Number of Particles	5000	10000	20000	35000
Time Costs (ms)	64	132	380	1034

time of processing each RSS measurement is calculated. The results with the particle number rising from 5000 to 35000 are listed in Table 5. As can be seen, with the particle number below 35000, the execution time of processing one RSS measurement is often below 1 s; it's obvious that as long as the RSS sampling interval is greater than 1 s, it is normally acceptable to have the particle number up to 35000. However, according to the aforementioned discussion in relation to the number of particles, having more than 10000 particles does not contribute to the estimation accuracy of the proposed algorithm. Therefore, it can be summarized that running the proposed algorithm on smartphones is feasible.

VI. CONCLUSION

In this paper, we presented a novel AP localization method by adopting the Rayleigh lognormal model and particle filtering. Differently from the well-known LDPL model, the Rayleigh lognormal model incorporates the pervasive small-scale fading (caused by the multipath effect). Moreover, we introduced PDR, PADAS, GPS in the outdoor case and WiFi fingerprinting in the indoor case to improve the practicality and accuracy of the proposed method. Indoor and outdoor experiments were carried out, and verified the effectiveness of the enhanced method. Finally, an Android APP was developed and confirmed the feasibility of the proposed method.

However, the proposed method is still restricted by the following limitations. First, only the 2-dimensional space is considered. Secondly, the localization accuracy of our method is dependent on the accuracy of any adopted localization technique, but their mathematical relationship is unknown. Therefore, we would like to advance our method by solving the above limitations in our future works.

ACKNOWLEDGMENT

This work was supported by the National Science and Technology Major Project of the Ministry of Science and Technology of China under Grant 2016YFB0502102, the National Natural Science Foundation of China under Grants 41871363, 41401519, 61761035 and 61461037, the Natural Science Foundation of Inner Mongolia Autonomous Region of China under Grant 2017JQ09, and the "Grassland Elite" Project of the Inner Mongolia Autonomous Region under Grant CYYC5016.

REFERENCES

[1] Y. Sun, M. Liu, and M. Q.-H. Meng, "WiFi signal strength-based robot indoor localization," in *Proc. IEEE Int. Conf. Inf. Automat. (ICIA)*, Jul. 2014, pp. 250–256. doi: 10.1109/ICInfA.2014.6932662.

[2] B. Huang, L. Xie, and Z. Yang, "TDOA-based source localization with distance-dependent noises," *IEEE Trans. Wireless Commun.*, vol. 14, no. 1, pp. 468–480, Jan. 2015. doi: 10.1109/TWC.2014.2351798.

[3] B. Huang, Z. Xu, B. Jia, and G. Mao, "An online radio map update scheme for wifi fingerprint-based localization," *IEEE Internet Things J.*, to be published. doi: 10.1109/JIOT.2019.2912808.

[4] H. Zou, B. Huang, X. Lu, H. Jiang, and L. Xie, "A robust indoor positioning system based on the procrustes analysis and weighted extreme learning machine," *IEEE Trans. Wireless Commun.*, vol. 15, no. 2, pp. 1252–1266, Feb. 2016. doi: 10.1109/TWC.2015.2487963.

[5] H. Zhao, B. Huang, and B. Jia, "Applying Kriging interpolation for WiFi fingerprinting based indoor positioning systems," in *Proc. IEEE Wireless Commun. Netw. Conf. (WCNC)*, Apr. 2016, pp. 1–6. doi: 10.1109/WCNC.2016.7565018.

[6] Y. Zhuang, Z. Syed, J. Georgy, and N. El-Sheimy, "Autonomous smartphone-based WiFi positioning system by using access points localization and crowdsourcing," *Pervas. Mobile Comput.*, vol. 18, pp. 118–136, Apr. 2015.

[7] B. Jia, B. Huang, H. Gao, W. Li, and L. Hao, "Selecting critical WiFi APs for indoor localization based on a theoretical error analysis," *IEEE Access*, vol. 7, pp. 36312–36321, 2019. doi: 10.1109/ACCESS.2019.2905372.

[8] Z. Yang, Z. Zhou, and Y. Liu, "From RSSI to CSI: Indoor localization via channel response," *ACM Comput. Surv.*, vol. 46, no. 2, p. 25, Dec. 2013.

[9] H. Lim, L.-C. Kung, J. C. Hou, and H. Luo, "Zero-configuration, robust indoor localization: Theory and experimentation," in *Proc. IEEE INFOCOM*, Apr. 2006, pp. 1–12. doi: 10.1109/INFOCOM.2006.223.

[10] J. Wang, J. Luo, S. J. Pan, and A. Sun, "Learning-based outdoor localization exploiting crowd-labeled WiFi hotspots," *IEEE Trans. Mobile Comput.*, vol. 18, no. 4, pp. 896–909, Apr. 2019. doi: 10.1109/TMC.2018.2849416.

[11] M. A. A. Rahman, M. Dashti, and J. Zhang, "Localization of unknown indoor wireless transmitter," in *Proc. Int. Conf. Localization GNSS (ICL-GNSS)*, Jun. 2013, pp. 1–6. doi: 10.1109/ICL-GNSS.2013.6577270.

[12] S.-M. Chun, S.-M. Lee, J.-W. Nah, J.-H. Choi, and J.-T. Park, "Localization of Wi-Fi access point using smartphone's gps information," in *Proc. Int. Conf. Sel. Topics Mobile Wireless Netw. (iCOST)*, Oct. 2011, pp. 121–126. doi: 10.1109/iCOST.2011.6085822.

[13] Y. Zhuang, Y. Li, H. Lan, Z. Syed, and N. El-Sheimy, "Wireless access point localization using nonlinear least squares and multi-level quality control," *IEEE Wireless Commun. Lett.*, vol. 4, no. 6, pp. 693–696, Dec. 2015. doi: 10.1109/LWC.2015.2483509.

[14] M. Ji, J. Kim, Y. Cho, Y. Lee, and S. Park, "A novel Wi-Fi ap localization method using Monte Carlo path-loss model fitting simulation," in *Proc. IEEE 24th Annu. Int. Symp. Pers., Indoor, Mobile Radio Commun. (PIMRC)*, Sep. 2013, pp. 3487–3491. doi: 10.1109/PIMRC.2013.6666752.

[15] Y. Zhuang, Y. Li, H. Lan, Z. Syed, and N. El-Sheimy, "Smartphone-based WiFi access point localisation and propagation parameter estimation using crowdsourcing," *Electron. Lett.*, vol. 51, no. 17, pp. 1380–1382, Aug. 2015. doi: 10.1049/el.2015.1724.

[16] A. Savvides, C.-C. Han, and M. B. Strivastava, "Dynamic fine-grained localization in ad-hoc networks of sensors," in *Proc. 7th Annu. Int. Conf. Mobile computing Netw.*, pp. 166–179, Jul. 2001.

[17] T. S. Rappaport *et al.*, *Wireless Communications: Principles and Practice*, vol. 2. Upper Saddle River, NJ, USA: Prentice-Hall, 1996.

[18] J. Koo and H. Cha, "Localizing WiFi access points using signal strength," *IEEE Commun. Lett.*, vol. 15, no. 2, pp. 187–189, Feb. 2011. doi: 10.1109/LCOMM.2011.121410.101379.

[19] S. Y. Nam, "Localization of access points based on signal strength measured by a mobile user node," *IEEE Commun. Lett.*, vol. 18, no. 8, pp. 1407–1410, Aug. 2014. 10.1109/LCOMM.2014.2332158.

[20] Z. Zhang, X. Zhou, W. Zhang, Y. Zhang, G. Wang, B. Y. Zhao, and H. Zheng. "I am the antenna: Accurate outdoor ap location using smartphones," in *Proc. 17th Annu. Int. Conf. Mobile Comput. Netw.*, Sep. 2011, pp. 109–120.

[21] X. Yang and B. Huang, "An accurate step detection algorithm using unconstrained smartphones," in *Proc. 27th Chin. Control Decis. Conf. (CCDC)*, May 2015, pp. 5682–5687. doi: 10.1109/CCDC.2015.7161816.

[22] B. HuaCng, G. Qi, X. Yang, L. Zhao, and H. Zou, "Exploiting cyclic features of walking for pedestrian dead reckoning with unconstrained smartphones," in *Proc. ACM Int. Joint Conf.*, Sep. 2016, pp. 374–385.

[23] I. M. Kostic, "Analytical approach to performance analysis for channel subject to shadowing and fading," *IEE Proc. Commun.*, vol. 152, no. 6, pp. 821–827, Dec. 2005. doi: 10.1049/ip-com:20045126.

[24] H. S. Qiang and J. Z. Liang, "Overview of particle filter algorithm," in *Control and Decision*. Shenyang, China, 2005.

[25] L. Zhao, N. Gao, B. Huang, Q. Wang, and J. Zhou, "A novel terrain-aided navigation algorithm combined with the TERCOM algorithm and particle filter," *IEEE J. Sensors*, vol. 15, no. 2, pp. 1124–1131, Feb. 2015. doi: 10.1109/JSEN.2014.2360916.

[26] J. Shen, B. Huang, X. Kang, B. Jia, and W. Li, "Localization of access points based on the Rayleigh lognormal model," in *Proc. IEEE Wireless Commun. Netw. Conf. (WCNC)*, Apr. 2018, pp. 1–6. doi: 10.1109/WCNC.2018.8377059.

[27] A. K. M. M. Hossain and W. Soh, "Cramer-rao bound analysis of localization using signal strength difference as location fingerprint," in *Proc. IEEE INFOCOM*, Mar. 2010, pp. 1–9. doi: 10.1109/INFCOM.2010.5462020.

[28] S. Venkatesh and R. M. Buehrer, "Multiple-access insights from bounds on sensor localization," in *Proc. Int. Symp. World Wireless, Mobile Multimedia Netw. (WoWMoM)*, Jun. 2006, p. 10. doi: 10.1109/WOWMOM.2006.77.

[29] F. Hansen and F. I. Meno, "Mobile fading—Rayleigh and lognormal superimposed," *IEEE Trans. Veh. Technol.*, vol. 26, no. 4, pp. 332–335, Nov. 1977. doi: 10.1109/T-VT.1977.23703.

[30] J. V. Candy, "Bootstrap particle filtering," *IEEE Signal Process. Mag.*, vol. 24, no. 4, pp. 73–85, Jul. 2007. doi: 10.1109/MSP.2007.4286566.

[31] S. H. Shin and C. G. Park, "Adaptive step length estimation algorithm using optimal parameters and movement status awareness," *Med. Eng. Phys.*, vol. 33, no. 9, pp. 1064–1071, Nov. 2011.

[32] A. Brajdic and R. Harle, "Walk detection and step counting on unconstrained smartphones," in *Proc. ACM Int. Joint Conf. Pervasive Ubiquitous Comput.*, Sep. 2013, pp. 225–234.

[33] X. Kang, B. Huang, and G. Qi, "A novel walking detection and step counting algorithm using unconstrained smartphones," *Sensors*, vol. 18, no. 1, p. E297, Jan. 2018.

[34] S. Han, Z. Gong, W. Meng, C. Li, D. Zhang, and W. Tang, "Automatic precision control positioning for wireless sensor network," *J. Sensors*, vol. 16, no. 7, pp. 2140–2150, Apr. 2016. doi: 10.1109/JSEN.2015.2506166.

[35] A. N. Bishop, B. Fidan, B. D. O. Anderson, K. Doğançay, and P. N. Pathirana, "Optimality analysis of sensor-target localization geometries," *Automatica*, vol. 46, no. 3, pp. 479–492, Mar. 2010.

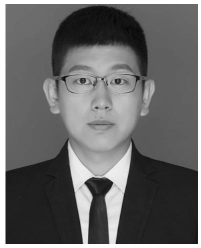

JUSHANG SHEN received the B.E. degree from Beijing Jiaotong University, Beijing, China, in 2016. He is currently pursuing the M.S. degree in computer science and technology from Inner Mongolia University, Hohhot, China. His research interest includes indoor location.

BAOQI HUANG received the B.E. degree in computer science from IMU, Hohhot, China, in 2002, the M.S. degree in computer science from Peking University, Beijing, China, in 2005, and the Ph.D. degree in information engineering from the Australian National University, Canberra, Australia, in 2012. From 2013 to 2014, he worked as Research Fellow with Nanyang Technological University, Singapore. He is currently a Professor with the College of Computer Science, IMU. He was a recipient of the Chinese Government Award for Outstanding Chinese Students Abroad in 2011. His research interests include wireless networks, sensor networks, mobile computing, ubiquitous computing, etc.

YU TIAN received the B.E. degree from Inner Mongolia University, Hohhot, China, in 2017. He is currently pursuing the M.S. degree in computer technology from Inner Mongolia University, Hohhot, China. His research interest includes indoor location.

LONG ZHAO received the B.E. degree from Inner Mongolia Normal University, Hohhot, China, in 1998, the M.S. degree from Harbin Engineering University, Harbin, China, in 2001, and the Ph.D. degree from Beihang University, Beijing, China, in 2004. His research interests include full source navigation, UAV navigation, pedestrian navigation, indoor location, etc.